82 ID 27 #2

67648

RESEARCH REPORT

EV-178

ABSOLUTE RATE CONSTANTS FOR THE REACTIONS OF OH RADICALS WITH ALKANES

Hydroxyl

Larry G. Anderson
Robert D. Stephens

Environmental Science Department

May 27, 1982

23 pages

GM
General Motors
Research Laboratories
Warren, Michigan 48090

RESEARCH REPORT NO. ● EV-178

Title ● Absolute Rate Constants for the Reactions of OH Radicals with Alkanes

Date ● May 27, 1982

Reported by ● Larry G. Anderson

Larry G. Anderson

Robert D. Stephens

Robert D. Stephens

Approved by ● Richard L. Klimisch

Richard L. Klimisch, Head
Environmental Science Department

General Motors Research Laboratories
Warren, Michigan 48090

PURPOSE

To investigate the kinetics of the hydroxyl radical (OH) reaction with alkanes over a wide temperature range.

SUMMARY

Alkanes may play an important role in the chain-carrying reactions which convert NO to NO_2 in both urban and rural atmospheres. In spite of the fact that the extent of participation of alkanes in these chain-carrying processes is controlled by the rate of OH attack, the kinetics of the OH-alkane reactions have received relatively limited attention. In addition, the bulk of the kinetic data on OH-alkane reactions does not cover the temperature region of atmospheric significance.

Kinetic results are presented in this report for the OH reaction with a series of alkanes. These results indicate that the rate constants for these OH - alkane reactions are smaller than previously reported. The principle reason for these discrepancies is believed to involve secondary reactions which affected the previously reported data. The secondary reactions resulted from the use of high initial OH radical concentrations in the previous studies. In the current work, some experiments were performed with high initial OH concentrations which demonstrate the importance of such secondary reactions. The kinetic data, reported here, was collected under conditions of low OH concentration where secondary reactions are not significant.

INTRODUCTION

Hydrocarbons play an important role in atmospheric chemistry. Hydrocarbons are involved in the chain-carrying reactions which oxidize NO to NO_2 in the atmosphere, as described by Demerjian et al.[1] The participation of hydrocarbons in these chain-carrying reactions is initiated by the reaction between hydrocarbons and the hydroxyl radical (OH). Calvert[2] has calculated the relative rates of OH radical reaction with the hydrocarbons measured in the Los Angeles atmosphere. He found that about 33% of the OH radicals reacting in the chaing-carrying steps react with alkanes, 35% with alkenes, 20% with aromatics, and 12% with CO. Clearly each of these classes of compounds plays a significant role in the conversion of NO to NO_2 in the urban atmosphere. Similar calculations of OH radical reactivity with hydrocarbons have been performed using rural hydrocarbon data collected in Rio Blanco, Colorado and the Smoky Mountains of Tennessee.[3] It is estimated that alkanes can account for 20-25% of the OH reaction with hydrocarbons in these rural areas.

The kinetics of hydroxyl radical reactions with alkanes have received little attention. With the exception of methane which has been widely studied and n-butane for which two temperature dependent studies have been reported, only one other study of the temperature dependence of OH - alkane reactions has been reported. All these alkane studies were at or above room temperature and did not extend below room temperature to the region of most importance in the atmosphere. The 1970 work of Greiner[4] reports the results of studies of the temperature dependent kinetics of a series of OH- alkane reactions using flash

photolysis-kinetic spectroscopic techniques. In that work, the initial OH radical concentration was assumed to be 3×10^{13} cm^{-3}, making it necessary to correct the measured kinetic data for the effects of possible secondary reactions. The corrections amounted to more than 30% of the reported rate constant in some cases. Clearly, significant uncertainty remains in our knowledge of the kinetics of OH - alkane reactions. A similar conclusion was reached in a recent review of the kinetics of OH radical reactions with organics.[5]

The purpose of the present study is to investigate the kinetics of a series of OH - alkane reactions over the temperature range from 250 to 370 K, which includes the range of interest in the atmosphere. The series of alkanes included in this study are ethane, propane, n-butane, isobutane and dimethylpropane. The kinetic studies were conducted at low initial OH radical concentrations to avoid complications due to secondary reactions involving OH.

EXPERIMENTAL

The discharge flow-resonance fluorescence apparatus used in this study is similar to that described previously.[6] In the current system an aluminum flow tube is used with eight fixed reactant injection ports at 5 cm intervals, corresponding to reaction distances between 10 cm and 45 cm. The walls of the flow tube were coated with a halocarbon wax (Series No. 15-00, Halocarbon Products Corp., Hackensack, New Jersey) to reduce the wall loss of OH radicals in the system.

Hydroxyl radicals were produced in the flow system by passing a dilute mixture of hydrogen in helium (typically 9 x 10^{-3}%) through a microwave discharge to form hydrogen atoms which react with NO_2 to produce OH radicals and NO. A large excess of NO_2 in helium was added to the flow a short distance downstream of the microwave discharge. Sufficient time was allowed for the reaction of H with NO_2 to go to completion and for vibrational deactivation of the vibrationally excited OH prior to entering the reaction zone. The OH radicals pass through the reaction zone, where reactant gases are added to the flow. Downstream of the reaction zone OH radicals are detected by resonance fluorescence. The detection system utilizes a resonance lamp consisting of a microwave discharge through a water/helium mixture for OH fluorescence detection. Fluorescence signals from the OH radicals in the flow system are detected by using an interference filter, photomultiplier and photon counting system.

The helium (99.999%), hydrogen/helium (92 ppm), nitrogen dioxide/helium (274 ppm) and alkane (99.5%, except ethane 99.0%) flows were controlled using calibrated mass flow controllers (Tylan). These gases were used without further purification. Gas chromatographic and gas chromatographic-mass spectrometric analyses of the alkanes indicated that the gases met the supplier's specifications and did not identify any complicating impurities.

The inital OH radical concentration used in the reaction studies was determined by one of two techniques. In the first of these techniques, the H atoms from the microwave discharge are titrated by the

addition of varying flows of NO_2 while monitoring the OH fluorescence signal. At the endpoint of the titration, the NO_2 flow is equivalent to the H atom flow at the point of NO_2 addition. The initial OH concentration is determined by assuming the complete conversion of H atams to OH in the presence of an excess of NO_2. The second technique for determining the initial OH concentration is based upon a calibration curve for the OH fluorescence signal versus OH concentration. The calibration curve is generated by monitoring the OH fluorescence signal resulting from the addition of a measured flow of NO_2 to an excess of H atoms. The OH concentration is assumed to be limited by the added NO_2. The concentration of OH was determined daily, or whenever the OH concentration was changed. The initial OH concentrations determined by these two techniques were in reasonable agreement and were typically 1-3 x 10^{11} cm^{-3}.

The wall loss rates for OH radicals in the flow system were determined using two different techniques. The first of these techniques used the addition of NO_2 through the eight fixed reactant injectors instead of near the discharge. The OH, thus formed, was exposed to the reactor walls for different distances (or times). By measuring the decay of OH fluorescence as a function of increasing distance, the first-order wall loss was determined. These wall loss rates were consistently less than 5 s^{-1}. This technique assumes the instantaneous formation of OH upon the addition of NO_2 to the H atoms in the flow tube and that the H atom wall loss in the flow tube is negligible. The errors introduced in the OH wall loss rate determination due to the finite time required for OH formation and a nonnegligible H atom wall loss rate both lead to underestimation of the OH wall loss rate. The

underestimation is partially compensated by the OH reaction with excess NO_2,[6] which contributes an additional OH loss of less than 1 s^{-1} under these experimental conditions.

The second method for estimating the OH wall loss rate uses a plot of pseudo-first-order rate constant data versus reactant concentration. The intercept of these plots provides a measure of the OH wall loss, assuming no reactant dependent surface loss. Sridharan et al.[7] have discussed some of the problems of determining OH wall loss rates in discharge flow systems. These problems are related to the use of moveable injectors for reactant addition, which leads to changes in the surface area for OH loss. However, a system using fixed injector ports does not have this problem. Since the surface to which OH is exposed is always the same. The OH wall loss rates determined from the intercept of the pseudo-first-order rate constant data versus reactant concentration were consistently higher than that determined by the addition of NO_2 through the injectors but were generally less than 10 s^{-1}. Both a reactant dependent wall loss and the reaction of OH with excess NO_2 may contribute to this measurement of the OH wall loss. However, the stable and low wall loss rates for OH in this system suggest that the kinetic data is not significantly influenced by these OH loss problems.

RESULTS

The initial OH radical concentration was measured to be in the range of 1-3 x 10^{11} cm^{-3} for all of the kinetic experiments reported.

No effects of secondary reactions were identified at these low OH radical concentrations. As will be discussed later, effects of secondary reactions were identified at higher initial OH concentrations.

Figure 1 shows a plot of some of the experimental data for the OH - n-butane reaction at 250 K. This figure shows the OH fluorescence decay as a function of reaction time for four of the n-butane concentrations used in this study. The slopes of these decay curves give a value for the pseudo-first-order rate constant for the OH - n-butane reaction at each of the n-butane concentrations. The measured pressure and calculated velocity were corrected for viscous pressure drop to derive the pressure and velocity at the average of the midpoints between reactant injection and OH detection. These corrections were typically about 5%. The axial diffusion corrections to the rate constants were less than 2% and were neglected. The bimolecular rate constants for the OH -alkane reactions were determined from plots of the pseudo-first-order rate constants, as determined above, versus the reactant alkane concentration. Figure 2 shows plots of such data for the five temperatures over which the OH - n-butane reaction was studied. The slope of each of these lines gives the bimolecular rate constant for the OH - n-butane reaction at the corresponding temperature. The intercepts of these lines provide one measure of the OH wall loss rate in these experiments.

Table 1 presents a summary of the rate data collected in 266 experiments for the reactions of OH radicals with the alkanes. Figure 3 shows an Arrhenius plot of the temperature dependence of the bimolecular rate constants determined for each of the five alkanes. The resulting

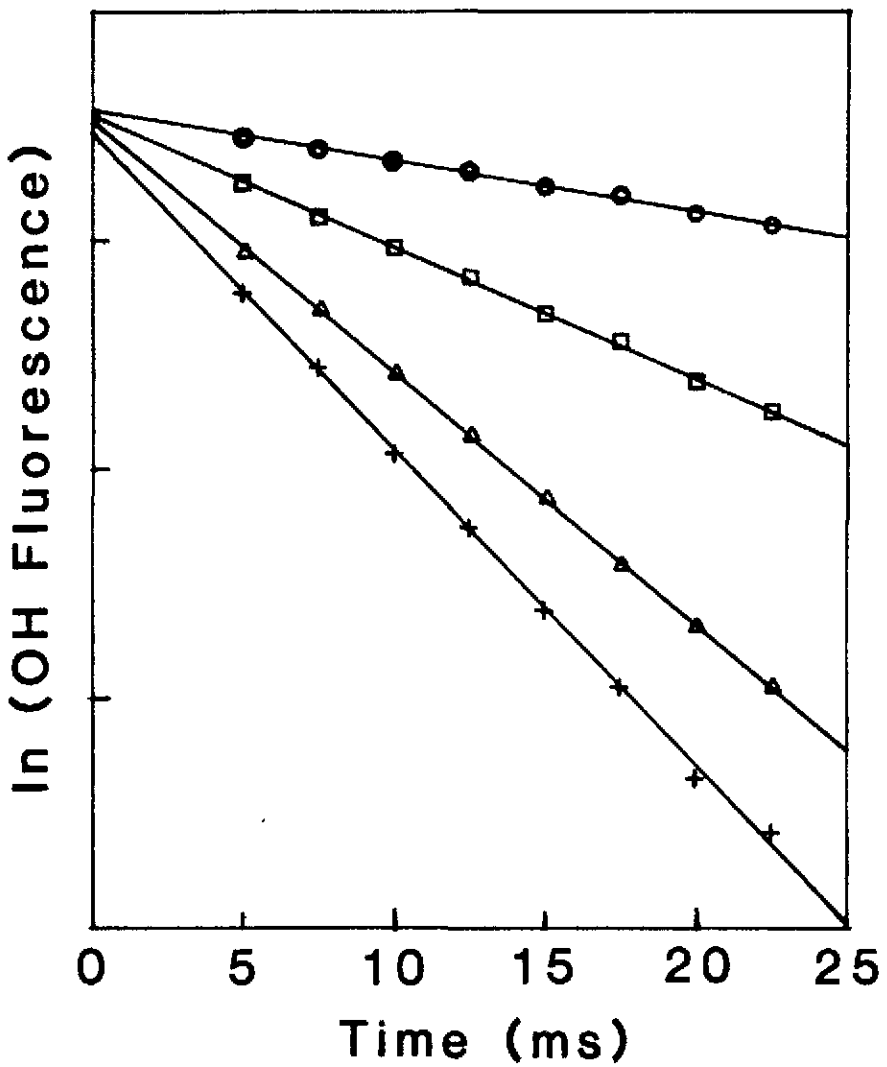

Figure 1. Plot of OH fluorescence decay data for the OH-n-butane reaction at 250 K. The four decay curves shown correspond to n-butane concentrations of: 1.18×10^{13}, 3.55×10^{13}, 7.05×10^{13} and 9.38×10^{13} molecule cm^{-3}, respectively, from top to bottom.

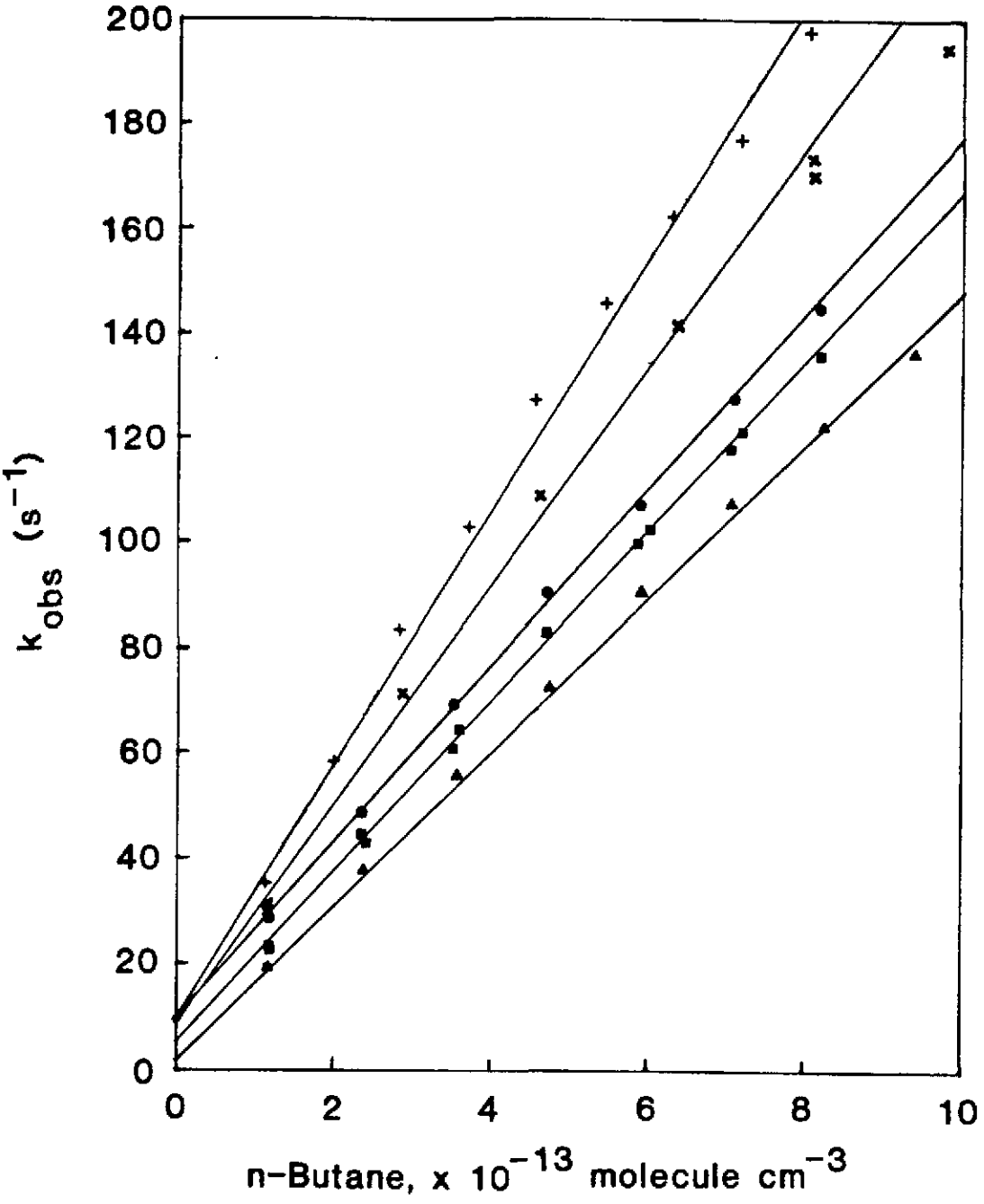

Figure 2. Plot of the pseudo-first-order rate constant for OH decay versus n-butane concentration for the five temperatures used in this study: 365 K, 329 K, 297 K, 274 K and 250 K, from the upper to the lower curve.

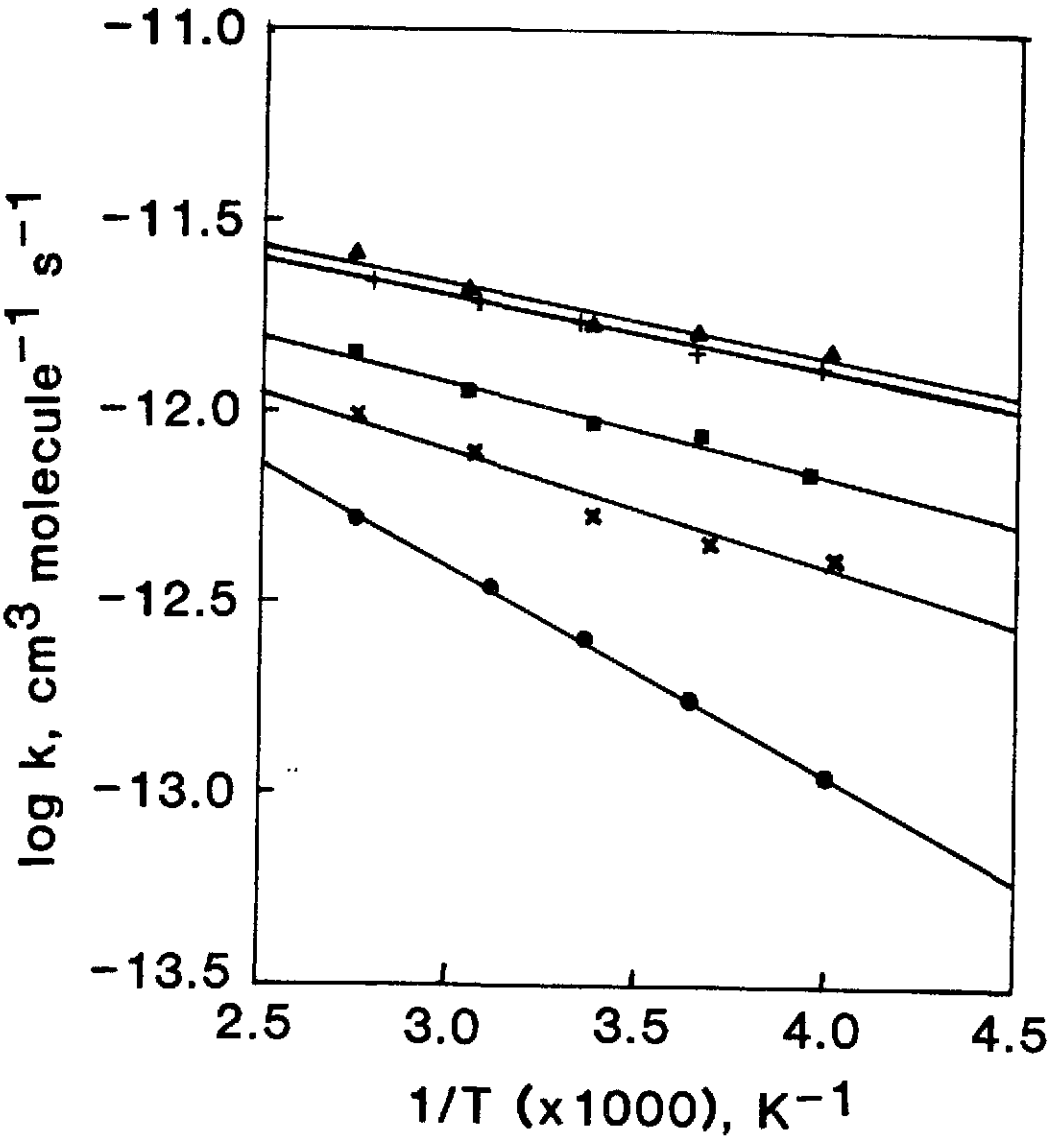

Figure 3. Arrhenius plots for the temperature dependence of the OH reaction rate constants with the alkanes : ● -ethane, ■ -propane, ▲ -n-butane, + -i-butane and ✖ -dimethylpropane.

Table I. Summary of OH-alkane rate constant data.

Reactant	Temp., K	No. of expts.	Pressure, torr	Concentration Range, molecule cm^{-3}	k_{bi},[a] cm^3 molecule^{-1} s^{-1}	Intercept,[b] s^{-1}
Ethane	250	17	1.07	$1.97 - 15.41 \times 10^{14}$	$(1.12\pm0.18)\times10^{-13}$	8.46±2.98
	275	7	1.12	$1.33 - 9.36 \times 10^{14}$	$(1.76\pm0.22)\times10^{-13}$	6.66±1.38
	298	23	1.00-1.16	$1.02 - 9.31 \times 10^{14}$	$(2.57\pm0.31)\times10^{-13}$	6.59±2.06
	322	10	1.04	$0.76 - 6.30 \times 10^{14}$	$(3.49\pm0.51)\times10^{-13}$	6.25±4.74
	364	7	1.02	$0.73 - 4.30 \times 10^{14}$	$(5.26\pm0.80)\times10^{-13}$	7.19±5.88
Propane	253	10	1.02	$0.40 - 3.03 \times 10^{14}$	$(6.86\pm1.07)\times10^{-13}$	14.91±5.88
	273	9	1.01	$0.38 - 2.33 \times 10^{14}$	$(8.79\pm1.23)\times10^{-13}$	11.56±3.92
	297	10	1.00	$0.16 - 1.59 \times 10^{14}$	$(9.29\pm1.21)\times10^{-13}$	2.12±1.58
	329	10	1.00-2.00	$0.16 - 1.39 \times 10^{14}$	$(11.26\pm1.63)\times10^{-13}$	3.92±2.38
	365	10	1.00	$0.15 - 1.54 \times 10^{14}$	$(14.09\pm1.95)\times10^{-13}$	5.86±3.30
n-Butane	250	22	1.00	$1.15 - 11.73 \times 10^{13}$	$(1.46\pm0.22)\times10^{-12}$	1.57±3.00
	274	12	1.00-2.00	$1.17 - 8.19 \times 10^{13}$	$(1.63\pm0.21)\times10^{-12}$	5.00±1.88
	297	7	1.00	$1.17 - 8.18 \times 10^{13}$	$(1.68\pm0.23)\times10^{-12}$	9.87±2.54
	329	9	1.02	$1.15 - 11.53 \times 10^{13}$	$(2.10\pm0.34)\times10^{-12}$	8.73±4.10
	365	15	1.05-2.11	$1.14 - 8.08 \times 10^{13}$	$(2.57\pm0.38)\times10^{-12}$	9.64±4.48
i-Butane	251	9	1.00	$2.22 - 11.03 \times 10^{13}$	$(1.31\pm0.19)\times10^{-12}$	11.09±2.68
	274	11	1.00	$1.11 - 9.89 \times 10^{13}$	$(1.46\pm0.19)\times10^{-12}$	9.90±1.80
	299	9	1.00	$1.09 - 9.87 \times 10^{13}$	$(1.73\pm0.25)\times10^{-12}$	3.84±2.28
	326	9	1.00-2.01	$1.10 - 8.89 \times 10^{13}$	$(1.95\pm0.25)\times10^{-12}$	9.99±2.18
	360	7	1.00	$1.10 - 6.64 \times 10^{13}$	$(2.21\pm0.39)\times10^{-12}$	5.92±4.84
Dimethylpropane	249	8	1.00	$0.51 - 3.23 \times 10^{14}$	$(4.14\pm0.71)\times10^{-13}$	1.07±2.22
	271	8	1.00	$0.43 - 2.91 \times 10^{14}$	$(4.60\pm0.89)\times10^{-13}$	4.39±3.26
	296	9	1.00-2.00	$0.43 - 2.39 \times 10^{14}$	$(5.33\pm0.98)\times10^{-13}$	10.57±3.90
	327	8	1.00	$0.26 - 1.91 \times 10^{14}$	$(7.72\pm1.53)\times10^{-13}$	5.68±3.28
	364	10	1.00	$0.17 - 1.37 \times 10^{14}$	$(9.87\pm2.31)\times10^{-13}$	8.29±6.18

[a] The error limits are the sum of the statistical uncertainty (± 2σ) and the systematic error estimate.

[b] The error limits are ±2σ values from the least squares fit.

Arrhenius parameters are presented in Table II. The systematic errors in this study were based on a detailed evaluation of the errors in each of the fundamental measurements contributing to the rate constant determination. The error limits on the rate constants reported throughout this paper are the sum of the systematic errors (10-13%) and two standard deviations, which represent the statistical uncertainty.

Some experiments were performed using high initial OH concentrations (8-10 x 10^{11} cm^{-3}). Figure 4 shows the data from two OH - n-butane experiments. These experiments were performed under identical conditions of pressure, velocity, temperature (250 K) and concentration, except for the difference in the initial OH concentration. The linear plot (upper) corresponds to the OH decay when the initial OH concentration was in the typical range (1-3 x 10^{11} cm^{-3}), while the lower curve is for the higher initial OH concentration. The curvature which is apparent at high OH is presumably due to secondary reactions. This curvature appeared to be less important at higher temperatures. The processes occurring at high OH concentration are expected to be the reaction of OH with n-butane and, since sufficient product (s-butyl radical) is formed, the secondary reaction of OH with the product s-butyl radical.

$$OH + n\text{-}C_4H_{10} \rightarrow H_2O + s\text{-}C_4H_9 \qquad (1)$$

$$OH + s\text{-}C_4H_9 \rightarrow \text{Products} \qquad (2)$$

At low OH concentrations, the primary reaction (1) is the only OH reaction of significance. For high initial OH concentrations, the data at low

Table II. Comparison of the kinetics results for the OH-alkane reactions.

Compound	k_{298}, cm^3 $molecule^{-1}$ s^{-1}	Temperature Range, K	Arrhenius Expression,[a] cm^3 $molecule^{-1}$ s^{-1}	Technique[b]	Reference
Ethane	$(2.83\pm0.45)\times10^{-13}$	297-493	$(1.86\pm0.30)\times10^{-11}\exp(-1231\pm53)/T$	FP-KS	4
	$(2.64\pm0.17)\times10^{-13}$			FP-RA	8
	$(2.90\pm0.60)\times10^{-13}$			DF-LMR	12
	$(2.57\pm0.31)\times10^{-13}$	250-364	$(1.64\pm0.26)\times10^{-11}\exp(-1245\pm46)/T$	DF-RF	This work
Propane	$(1.20\pm0.11)\times10^{-12}$	296-497	$(1.19\pm0.13)\times10^{-11}\exp(-678\pm38)/T$	FP-KS	4
	$(0.83\pm0.17)\times10^{-12}$			DF-ESR	13
	$(2.02\pm0.10)\times10^{-12}$			FP-RA	8
	$(0.93\pm0.12)\times10^{-12}$	253-365	$(6.21\pm2.37)\times10^{-12}\exp(-552\pm113)/T$	DF-RF	This work
n-Butane	$(2.57\pm0.12)\times10^{-12}$	298-495	$(1.42\pm0.35)\times10^{-11}\exp(-524\pm93)/T$	FP-KS	4
	4.1×10^{-12}			DF-MS	9
	$(2.35\pm0.35)\times10^{-12}$			FP-RF	14
	$(2.72\pm0.27)\times10^{-12}$	298-420	$1.76\times10^{-11}\exp(-560\pm150)/T$	FP-RF	11
	$(2.67\pm0.22)\times10^{-12}$			FP-RA	10
	$(1.68\pm0.23)\times10^{-12}$	250-365	$(8.17\pm4.03)\times10^{-12}\exp(-443\pm143)/T$	DF-RF	This work
i-Butane	$(2.46\pm0.25)\times10^{-12}$	297-498	$(8.78\pm1.69)\times10^{-12}\exp(-387\pm63)/T$	FP-KS	4
	$(1.73\pm0.25)\times10^{-12}$	251-360	$(7.67\pm1.12)\times10^{-12}\exp(-448\pm42)/T$	DF-RF	This work
Dimethylpropane	$(8.25\pm0.73)\times10^{-13}$	292-493	$(1.42\pm0.19)\times10^{-11}\exp(-844\pm44)/T$	FP-KS	4
	$(9.10\pm0.98)\times10^{-13}$			FP-RA	10
	$(5.33\pm0.98)\times10^{-13}$	249-364	$(6.03\pm4.11)\times10^{-12}\exp(-684\pm187)/T$	DF-RF	This work

[a] The error limits reported for the Arrhenius parameters from this work are the $\pm2\sigma$ values determined from the weighted least squares fit of the data.

[b] OH production: FP, flash photolysis; DF, discharge flow. OH detection: KS, kinetic spectroscopy; RA, resonance absorption; LMR, laser magnetic resonance; RF, resonance fluorescence; ESR, electron spin resonance; MS, mass spectroscopy.

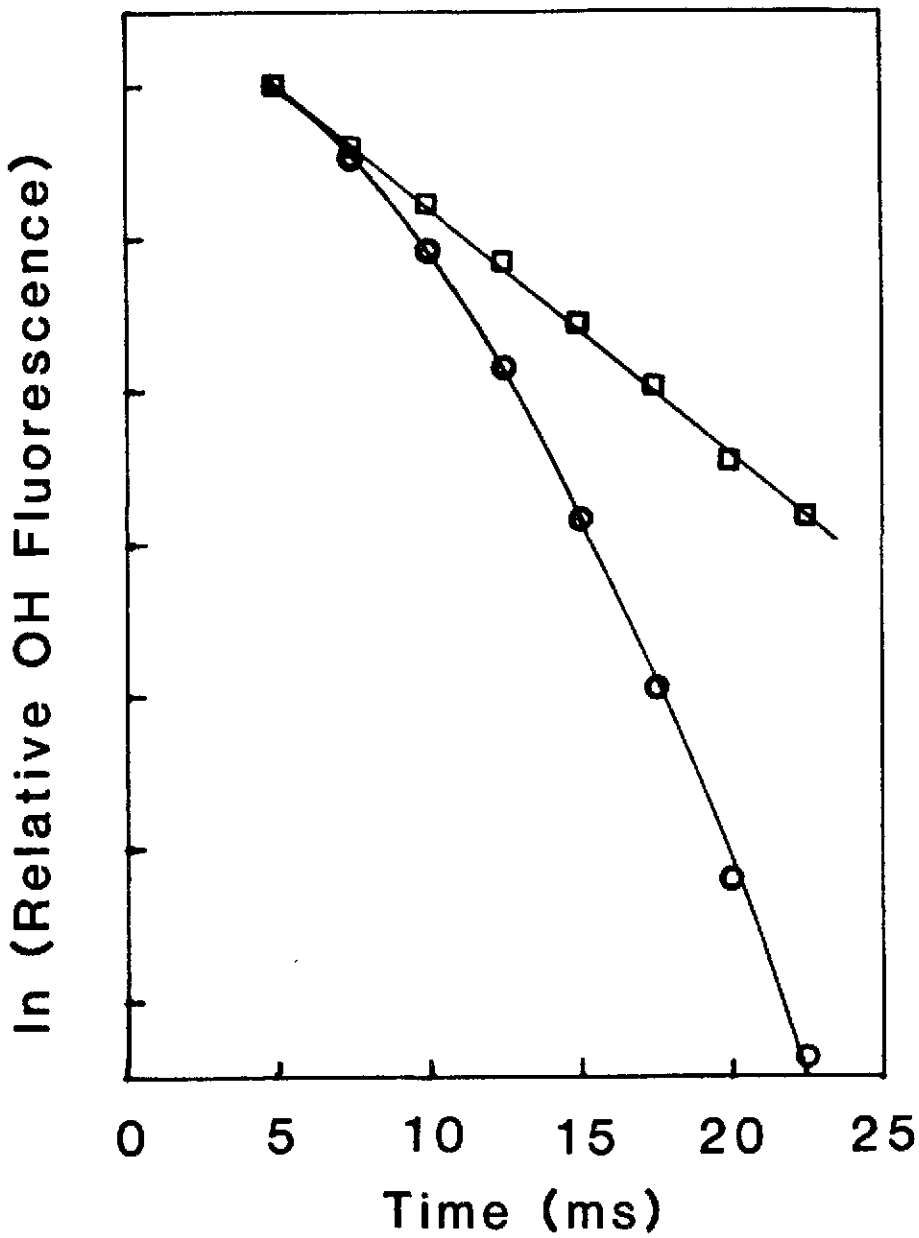

Figure 4. Plots of the OH fluorescence decay for the reaction with n-butane at 250 K. The upper curve shows the data resulting from experiments with an initial OH concentration of about 2×10^{11} cm^{-3} and n-butane, 1.18×10^{13} molecule cm^{-3}, while the lower curve is for a higher initial OH concentration of about 9×10^{11} cm^{-3} and n-butane, 1.23×10^{13} molecule cm^{-3}.

n-butane concentration gives an OH decay rate about twice that for low OH concentrations. As the n-butane concentration is increased, the ratio of the OH decay rate at high OH to the OH decay rate at low OH decreases. This behavior is consistent with the modeling of radical-radical reaction effects performed by Overend et al.[8] Throughout the course of the OH - alkane studies, the initial OH concentration was varied to be certain that radical-radical effects were not included in the kinetic data presented in this work.

DISCUSSION

A comparison of the results in this study with previously published rate data for OH - alkane reactions is shown in Table II. The present room temperature rate data agrees reasonably well with the other direct determinations of the OH - alkane rate constants, although they are generally lower than previously reported. In the cases of ethane, propane and n-butane almost all of the data agrees to within 25% of current results. Only the data of Overend et al.[8] for propane and Morris and Niki[9] for n-butane are outside this range. In the work of Overend et al.[8], the initial OH concentration was near 3×10^{13} cm^{-3}, about two orders of magnitude higher than used in the current experiments. They attempted to correct their work for the effects of secondary reactions, but that correction appears to have been inadequate, since their results are about twice those of other direct kinetic studies of this reaction. The OH - n-butane results of Morris and Niki[9] are based on a limited number of studies using a rather crude kinetic

analysis. Again, their results are almost twice those reported in five other room temperature studies. For OH + isobutane and OH + dimethylpropane, the room temperature kinetic results vary by 30 to 35% from the results reported previously. In both cases, the initial OH concentrations used in previous studies were near 3×10^{13} cm^{-3}.[4,10] Greiner[4] recognized that interferences from secondary reactions could play a significant role in the OH loss kinetics and made corrections to his data averaging 13% and 14% for isobutane and dimethylpropane, respectively. Paraskevopoulos and Nip[10] used initial OH concentrations in the range $2.4\text{-}4.8 \times 10^{13}$ cm^{-3} in studies of the OH reaction with dimethylpropane, but no correction for secondary effects on the OH - dimethylpropane kinetics were made. It is believed that the discrepancy between the previously reported results and these results for the OH reactions with isobutane and dimethylpropane are due to secondary reactions in the previous studies.

The current temperature dependent results show a consistently lower activation energy than previously reported (Table II), with the exception of the isobutane results. The result for ethane, propane and n-butane agree with the results for previous studies to within an average of 25% for the temperature regions where the current studies overlap with previous studies. Since the temperature dependent studies of the OH - alkane reactions were those of Greiner[4] who used a high initial OH concentration, the discrepancies between the current and previous results are believed to be due to complications resulting from secondary reactions. Perry et al.[11] have also reported temperature dependent results for the OH - n-butane reaction that are higher than those determined in

this work. Since they used the flash photolysis-resonance fluorescence technique presumably with low initial OH concentrations, secondary reactions are not expected to be of significance. The fit to the current data is in reasonable agreement (within 25%) with the rate data from Perry et al.[11] in the region in which the temperature ranges of the two studies overlap.

The OH - alkane data from the current work was analyzed by a technique similar to Greiner's[4] to apportion the OH reactivity with each alkane to the abstraction of primary, secondary or tertiary H atoms. Figure 5 shows the resulting Arrhenius plots for OH abstraction of primary, secondary and tertiary H atoms from the alkanes. The rate constant for primary H atom abstraction, k_p, was determined from the data for ethane (6 primary H atoms) and dimethylpropane (12 primary H atoms). The resulting curve shown in figure 5 for k_p is based on an Arrhenius fit to the data for the two alkanes on a per primary H atom basis. The rate constant for abstraction of tertiary H atoms, k_t, was based upon the isobutane data (1 tertiary H atom) after the reactivity due to the 9 primary H atoms was subtracted. Table III shows a comparison between the Arrhenius expressions for primary, secondary and tertiary H atoms from this work with those derived by Greiner.[4] Greiner's[4] values were based on fits to a larger set of OH - alkane data than were the current values. The comparison between the two studies is reasonably good considering the problems with secondary reactions mentioned above.

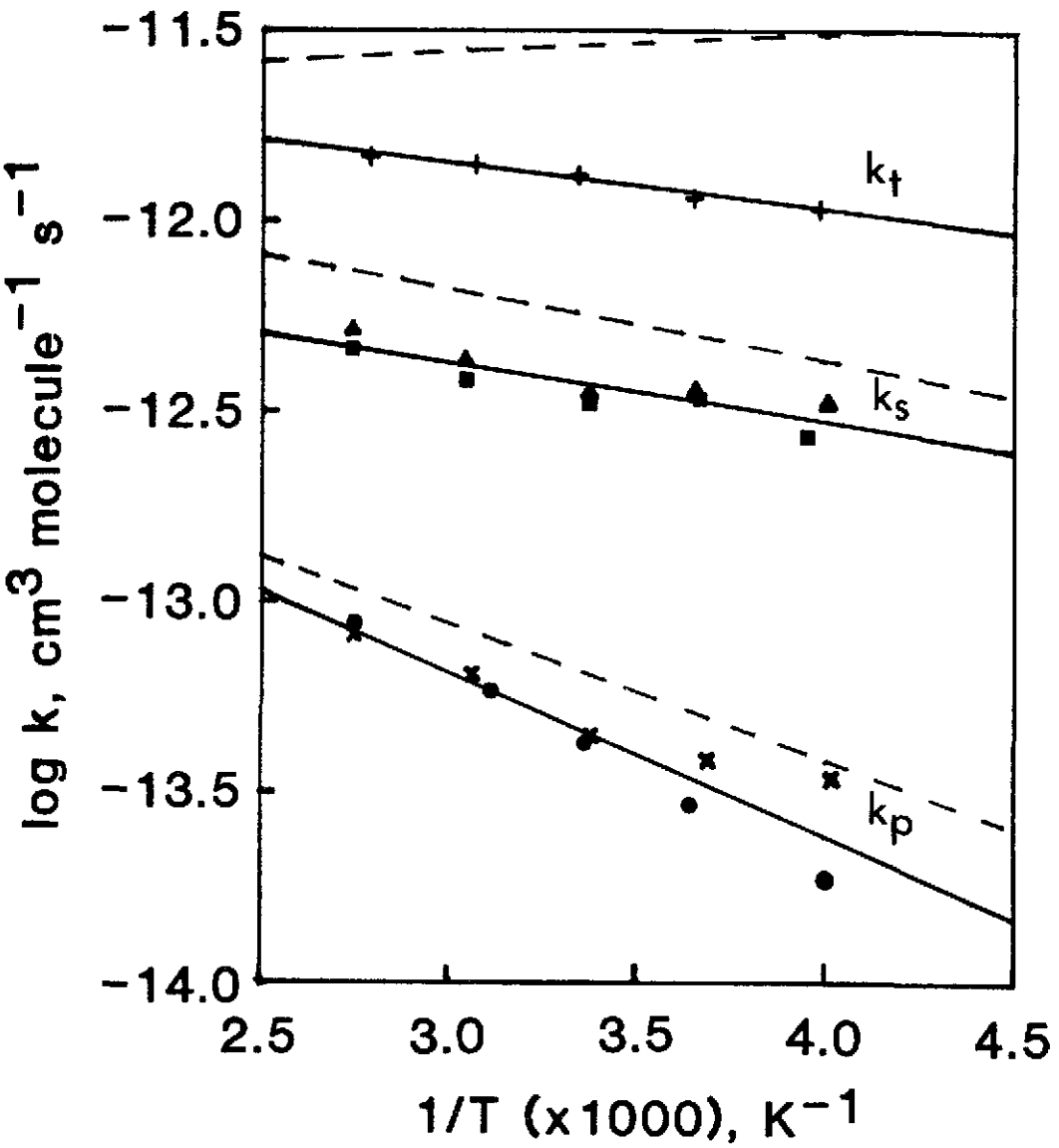

Figure 5. Arrhenius plots for the temperature dependence of the OH abstraction reactions of primary (k_p), secondary (k_s) and tertiary (k_t) H atoms from alkanes. These rate constants are determined as described in the text and are based upon the alkanes: ●-ethane, ■-propane, ▲-n-butane, +-i-butane and ✖-dimethylpropane. The dashed lines represent the results of Greiner's[4] determination of these rate constants.

Table III. Comparison of Arrhenius expressions for the abstraction of primary, secondary and tertiary H atoms from alkanes by the OH radical.

H Abstraction	k, cm^3 $molecule^{-1}$ s^{-1}	Reference
Primary	$1.02 \times 10^{-12} \exp(-823/T)$	4
	$(1.30 \pm 0.61) \times 10^{-12} \exp(-1001 \pm 138)/T$	This work
Secondary	$2.35 \times 10^{-12} \exp(-428/T)$	4
	$(1.21 \pm 0.28) \times 10^{-12} \exp(-354 \pm 67)/T$	This work
Tertiary	$2.09 \times 10^{-12} \exp(+96/T)$	4
	$(3.31 \pm 0.28) \times 10^{-12} \exp(-281 \pm 25)/T$	This work

REFERENCES

1. K. L. Demerjian, J. A. Kerr and J. G. Calvert, Adv. Environ. Sci. Technol., 4, 1 (1974).
2. J. G. Calvert, Environ. Sci. Technol., 10, 256 (1976).
3. R. R. Arnts and S. A. Meeks, Atmos. Environ., 15, 1643 (1981).
4. N. R. Greiner, J. Chem. Phys., 53, 1070 (1970).
5. R. Atkinson, K. R. Darnall, A. C. Lloyd, A. M. Winer and J. N. Pitts, Adv. Photochem., 11, 375 (1979).
6. L. G. Anderson, J. Phys. Chem., 84, 2152 (1980).
7. U. C. Sridharan, B. Reimann and F. Kaufman, J. Chem. Phys., 73, 1286 (1980).
8. R. P. Overend, G. Paraskevopoulos and R. J. Cvetanovic, Can. J. Chem., 53, 3374 (1975).
9. E. D. Morris and H. Niki, J. Phys. Chem., 75, 3640 (1971).
10. G. Paraskevopoulos and W. S. Nip, Can. J. Chem., 58, 2146 (1980).
11. R. A. Perry, R. Atkinson and J. N. Pitts, J. Chem. Phys., 64, 5314 (1976).
12. C. J. Howard and K. M. Evenson, J. Chem. Phys., 64, 4303 (1976).
13. J. N. Bradley, W. Hack. K. Hoyermann and H. Gg. Wagner, J. Chem. Soc. Faraday Trans. 1, 69, 1889 (1973).
14. F. Stuhl, Z. Naturforsch., 28A, 1383 (1973).

DISTRIBUTION

Research Laboratories

C. S. Tuesday	Executive Department
F. E. Jamerson	Physics Department
J. G. Larson	Physical Chemistry
T. M. Sloane	" "

Technical Information Department (3)

Environmental Activities Staff

D. L. Boyd	Research Contact
S. W. Martens	

Patent Section

G. A. Grove